Paleoseismology of Sanak Island: Collaborative Research with University of Rhode Island, Rutgers University, and U.S. Geological Survey

External Grand Award Numbers: G14AP00081 and G14AP00080

Investigators: Simon Engelhart[1], Benjamin Horton[2], Tina Dura[2]

1. Department of Geosciences, University of Rhode Island, 336 Woodward Hall, 9 East Alumni Avenue, Kingston, RI 02881, USA, engelhart@uri.edu

2. Department of Marine and Coastal Science, Rutgers University, 71 Dudley Road, New Brunswick, NJ 08901, USA, bphorton@marine.rutgers.edu

Start date: July 1st 2014
End date: June 30th 2015

Research supported by the U.S. Geological Survey (USGS), Department of the Interior, under USGS award numbers ***G14AP00081 and G14AP00080****. The views and conclusions contained in this document are those of the authors and should not be interpreted as necessarily representing the official policies, either expressed or implied, of the U.S. Government.*

Abstract

We sampled four sites on southern and eastern facing aspects of Sanak Island: Dodds West; Dodds Valley; Sandy Bay South; and Salmon Bay. Field methods involved the use of gouge cores to undertake reconnaissance of stratigraphy. We collected core samples using Russian and Fat Gouge hand driven coring devices at core locations that were representative of the overall stratigraphy at each study site. Analysis of the cores resulted in us obtaining 19 new AMS radiocarbon dates and 57 samples documenting the diatom assemblages. We constructed island-wide correlations between the four sites in the field using two distinctive tephras: a fine-grained grey tephra; and a coarse-grained red to orange tephra. Subsequent AMS radiocarbon dating confirms our field correlations.

Suitable sites for identifying land-level changes could not be located on Sanak Island. However, we find evidence for marine incursions up to five times during the last 4500 years, including the 1946 AD earthquake. Evidence for marine incursion consists of sand deposits that are compositionally similar to beach sand that were deposited within late Holocene tephra-derived soil and marsh sequences at three sites (Dodds Bay/Dodds Valley/Salmon Bay) and within freshwater marsh peat at Sandy Bay South. Sand beds contain marine diatoms indicating a marine source. On the basis of elevation above modern sea level and extent of inundation, we conclude that these sand beds are most likely due to inundation by tsunami rather than storms.

Our stratigraphy and diatom data coupled with chronology from AMS C-14 ages demonstrate that at Sanak Island, where the megathrust is currently creeping, repeated tsunamis have inundated >500m inland and >4m above modern mean sea level during the last 4500 years. The relationship between apparent lack of coupling during the instrumental era and previous marine incursions is unclear.

Context

The Alaska-Aleutian megathrust is capable of producing Mw 9+ earthquakes and associated large tsunamis as evidenced by the 1964 Mw 9.2 earthquake. Results of almost two decades of GPS instrumentation coupled with increasingly sophisticated modeling are identifying previously unresolved patterns of deformation. However, because GPS measurements span only fractions of most earthquake cycles, many aspects of ongoing plate-deformation lack a unique interpretation. Little is known about the recurrence intervals and magnitudes of great earthquakes of the Alaska-Aleutian megathrust. Therefore, the seismic hazard posed by subduction zone faults can only be completely understood by studying paleoseismology records over many seismic cycles extending back hundreds to thousands of years.

Detailed paleoseismology records of the Alaska-Aleutian megathrust are limited to Cook Inlet and eastern Kodiak Island (areas only 400 km apart). These study sites are within the 1964 rupture area, which itself represents only 20% of the 3000 km Alaskan-Aleutian megathrust. Our study site, Sanak Island (Figure 1), is to the west of Kodiak Island. Sanak Island was inundated by the tsunami from the 1946 AD earthquake (e.g., Okal et al., 2003), and is within the hypothesized 1788 rupture zone (e.g., Lander et al., 1996). Indeed the 1946 "Scotch Cap" tsunami was the deadliest in US history, with more than 150 fatalities in Hawaii.

We therefore set out to evaluate the paleoseismic history of Sanak Island to address research questions including:

1. Are modern geodetic measurements consistent with the paleoseismology?

2. If evidence for earthquakes and/or tsunamis are found, what are the recurrence intervals for these events near Sanak Island?

Project deliverables included:

1. Collection of sediment cores from sites on Sanak Island to analyze evidence for land-level changes and/or tsunami deposits.

2. Analysis of fossil diatom samples.

3. Analysis of geochemistry samples.

4. Analysis of AMS C-14 dates and Cs-137 data to produce a chronology for earthquakes and/or tsunami at Sanak Island.

5. Presentation of results at scientific meetings.

6. Submission of results to peer-reviewed journals

1. Summary of deliverables

We sampled four sites on Sanak Island: Dodds West; Dodds Valley; Sandy Bay South; and Salmon Bay (Figure 1). Field methods involved the use of gouge cores to undertake reconnaissance of stratigraphy. We collected core samples using Russian and Fat Gouge hand driven coring devices at core sites that were representative of the overall stratigraphy at each site. Analysis of the cores resulted in us obtaining 19 new AMS radiocarbon dates and 57 samples documenting the diatom assemblages in and around anomalous sand beds. We tested whether a new geochemistry technique could distinguish between marine and terrestrial sources for the sands. We constructed island-wide correlations between the four sites in the field using two distinctive tephras: a fine-grained grey tephra; and a coarse-grained red to orange tephra. Subsequent AMS radiocarbon dating confirms our field correlations. We are presenting our initial findings at the 2015 Geological Society of America meeting in Baltimore and will submit a paper for peer review by May 2016.

2. Methods

2.1 Core Descriptions

Grain size, sedimentary structures, contacts, thickness, and lateral and vertical facies changes were described in the field using general stratigraphic methods in combination with the Troels-Smith (1955) method for describing organic-rich sediment.

2.2 Surveying to sea-level datum

Elevational accuracy is crucial for all our mapping and sampling. To establish vertical orthometric and tidal data at each site, we pursued two strategies. Firstly, we leveled cores, pits, and topographic elevations with a RTK GPS instrument. Data collected by the GPS base station was post-processed to obtain North American Vertical Datum 88 (NAVD88) orthometric elevations. To establish elevations with respect to a tidal datum, we installed water pressure sensors at Petersen Bay to capture the shape and timing of the tidal curve for comparison to the nearest tide gauge at Sand Point. We needed to use both orthometric and tidal-datum strategies because the link between NAVD88 orthometric and NOAA tidal data is not well established in Alaska (e.g., Kemp et al., 2013a).

2.3 Chronology

We picked plant macrofossil samples from selected cores for AMS ^{14}C dating (Table 1). We focused on samples that can tightly constrain the timing or tsunami sand deposition, such as tidal herb stems entombed in mud or sand and seeds from terrestrial plants (e.g., Kemp et al., 2013b). Multiple ^{14}C ages above and below key contacts related to land-level changes and tsunami deposits allow stratigraphic correlation among sites. We have decades of experience with this type of dating. We have developed age models for our stratigraphic sequences using Bayesian statistical software (BChron, Parnell et al., 2008). We used Cs-137 to ascertain the age of the upper sand at Dodds West, Dodds Valley, and Salmon Bay.

2.4 Diatoms
We conducted fossil diatom analysis to help characterize sand beds and determine sediment provenance (Hemphill-Haley, 1995; Dawson, 2007; Pilarczyk et al., 2014). We subsampled the stratigraphy of Core DW107A and Core DV103C at 1 cm intervals in the organic silts that bracket the sand beds and within the sand beds themselves. Diatoms were extracted from ~1 g of sediment using the standard preparation methods of Palmer and Abbott (1986). Between 25 and 100 mL (depending on the diatom concentration) of clean diatom solution was pipetted evenly on a cover slip, dried, and the coverslip mounted on a glass slide using Naphrax. A total of 50 diatom slides were prepared and counted. Diatoms were identified to species level using a light microscope under oil immersion at 1000x magnification with reference to Krammer and Lange-Bertalot (1986, 1988, 1991 a,b) and Lange-Bertalot (2000). When possible >200 diatoms were identified and counted in slides with each species expressed as a percentage of total diatom valves counted. We classified diatoms based on their salinity preference as outlined in Alaskan references (Zong et al., 2003; Hamilton and Shennan, 2005a,b; Shennan et al., 2007; Shennan et al., 2010) and global catalogs (Krammer and Lange-Bertalot, 1986, 1988, 1991 a,b; Hartley et al., 1986; Vos and de Wolf, 1988, 1993; Denys, 1991). Samples were also scanned for the abundance of chrysophyte cysts (freshwater golden algae) to help distinguish freshwater from tidal environments. In the diatom diagrams we show only those freshwater species >10% of the assemblage, and those marine species >2% of the assemblage.

2.5 Geochemistry
A relatively new organic geochemical approach based on the distribution of branched GDGTs (brGDGTs) compared to the one of crenarchaeol (isoprenoid GDGT) is tested to track tsunami sediment layers in cores from the Sanak Island. BrGDGTs are mainly produced by soil bacteria while crenarchaeol is a biomarker for marine Archaea of the genus Thaumarchaeota, although it has been reported cases of low amount of crenarchaeol production in soils (Schouten et al., 2013 and references therein). This proxy quantified in the so-called Branched and Isoprenoid Tetraether (BIT) index (Hopmans et al., 2004) have been used by several studies to track soil organic matter input into aquatic environments. BIT index values bellow ca. 0.3 are typical from marine environments whilst values closer to 1 are from a terrestrial environment. Here, we measure the BIT index and quantify the concentration of both, brGDGT and crenarchaeol, in 3 cores (DV102, 103 and 107B).

3. Results

3.1 Stratigraphy

3.1.1 Dodds West
Dodds West records evidence of five inundation events (DW1 through DW5) during the last ~4500 years (Figure 2).

3.1.2 Dodds Valley

Dodds Valley records evidence of four inundation events (DV1 through DV4) during the last 4500 years (Figure 3).

3.1.3 Sandy Bay South

Sandy Bay South records evidence of two inundation events (SBS1 and SBS2) during the last ~2000 years (Figure 4).

3.1.4 Salmon Bay

Salmon Bay records evidence of two inundation events (SB1 and SB2) during the last ~2000 years (Figure 5)

3.2 Chronological data

Our new AMS 14-C ages are shown in Table 1. We determine that Sand 1 was deposited by the 1946 AD earthquake, consistent with Cs-137 data (Figure 6) at three sites (Dodds Valley, Dodds West, Salmon Bay) that demonstrate deposition prior to 1963, "bathtub" rings of driftwood around the sites, and previous research that indicated inundation up to 6m at our sites during the 1946 earthquake that was greater than observed during the 1957 earthquake that occurred further west (Okal et al., 2003). Using the tephras and our 14-C ages, we correlate sands between sites as shown in Table 2. Estimated ages derived from Bayesian age modeling using Bchron (Parnell et al., 2008) of each sand layer are shown in Figure 7.

3.3 Diatom Analysis

3.3.1 Dodds West

Sand DW5

Samples from the organic silt below sand bed DW5 (Figure 8) contain well-preserved, abundant (>50%) marine tidal flat diatoms (e.g., *Cocconeis costata*, *Cocconeis scutellum*, and *Grammatophora marina*) and marine plankton (*Hyalodiscus scoticus* and *Thalassiosira* sp.) with lesser abundances (<50%) of freshwater marsh diatoms (*Pinnularia intermedia*, *Pinnularia lagerstedtii*) and chrysophyte cysts. The mixed tidal flat and freshwater assemblage is unique in that is does not contain any transitional, low marsh diatoms. It is possible that winter processes, such as a build-up of sediment-laden sea-ice on the tidal flat could have transported tidal flat diatoms onto the freshwater tidal marsh (Hamilton et al., 2005), creating the mixed assemblage. However it is difficult to distinguish winter processes from other processes contributing to mixed diatom assemblages, such as the daily tidal mixing that occurs throughout the year.

Marine tidal flat diatoms (e.g., *Cocconeis costata*, *Cocconeis scutellum*, and *Grammatophora marina*) and marine plankton (*Hyalodiscus scoticus* and *Thalassiosira* sp.) reach their highest abundance in the core (82%) in sand bed DW5.

The well-preserved assemblage includes the same taxa found below the sand, but is characterized by a decrease in freshwater microfossils and a high percent abundance of marine plankton (26%) compared to underlying sediments (15%) and overlying sediments (11%).

The organic silt immediately overlying sand bed DW5 contains abundant, well-preserved (>50%) marine tidal flat and marine planktonic diatoms with lesser abundances (<50%) of freshwater marsh diatoms and chrysophyte cysts, similar to sediments underlying sand bed DW5. Two centimeters above sand bed DW5, freshwater diatoms begin to increase and marine diatoms decrease, reflecting an environment with a decreased marine influence. The appearance of the freshwater diatom *Eunotia praerupta* 2 cm above sand bed DW5 supports a freshening system.

Sand DW4
Samples from the organic silt below sand bed DW4 (Figure 8) contain well-preserved, abundant freshwater diatoms (*Achnanthidium reimeri, Eunotia praerupta, Pinnularia brevicostata, Pinnularia intermedia*, and *Pinnularia lagerstedtii*) and chrysophyte cysts typical of a freshwater marsh environment. No marine taxa were found in samples underlying sand bed DW4, suggesting the winter or tidal processes responsible for the mixed assemblages in the base of the core are no longer acting on the freshwater marsh.

Diatoms within sand bed DW4 are characterized by high fragmentation, low concentration, and an influx of marine tidal flat diatoms (*Cocconeis scutellum* (16%), *Delphineis surirella* (11%), and *Cocconeis costata* (6%)) into an assemblage otherwise dominated by freshwater taxa. The fragmented, mixed assemblage containing anomalous tidal flat diatoms is consistent with a marine incursion into the freshwater marsh.

The tephra above sand bed DW4 contains no diatoms.

Sand DW3
Samples from the organic silt below sand bed DW3 (Figure 9) contain well-preserved, abundant freshwater diatoms (*Achnanthidium reimeri, Eunotia praerupta, Pinnularia brevicostata, Pinnularia intermedia*, and *Pinnularia lagerstedtii*) and chrysophyte cysts typical of a freshwater marsh environment. No marine taxa were found in samples underlying sand bed DW3.

Diatoms within sand bed DW3 are characterized by high fragmentation, low concentration, and an influx of marine tidal flat diatoms (*Delphineis surirella* (16%), *Planothidium delicatulum* (11%), *Cocconeis scutellum* (6%)) into an assemblage otherwise dominated by freshwater taxa. We also observed an increase in freshwater diatoms commonly found in shallow lakes and ponds (*Platessa hustedtii*, *Stauroforma exiguiformis, Staurosira construens*) in the sand. The fragmentation of diatom valves, and the anomalous tidal flat diatoms and shallow freshwater diatoms in sand bed DW3 are consistent with a tsunami eroding, transporting, and depositing sediments from a variety of environments.

The organic silt immediately overlying sand bed DW3 contains well-preserved, abundant freshwater diatoms and chrysophyte cysts typical of a freshwater marsh environment, similar to sediments below sand bed 3. Two samples from the “Red beard” tephra (samples 33-34 cm and 34-35 cm) contain few (<100) diatoms, but those present are consistent with the freshwater marsh assemblage found in underlying and overlying samples. No marine taxa were found in samples overlying sand bed DW3.

Sand DW2

Samples from the organic silt immediately below sand bed DW2 (Figure 9) contain well-preserved, abundant freshwater diatoms (*Achnanthidium reimeri, Eunotia praerupta, Pinnularia brevicostata, Pinnularia intermedia*, and *Pinnularia lagerstedtii*) and chrysophyte cysts typical of a freshwater marsh environment. No marine taxa were found in samples underlying sand bed DW2.

Diatoms within sand bed DW2 are characterized by high fragmentation, low concentration, and an influx of marine tidal flat diatoms (*Planothidium delicatulum* (6%), *Cocconeis scutellum* (5%), *Grammatophora marina* (5%)) into an assemblage otherwise dominated by freshwater taxa. We also observed an increase in freshwater diatoms commonly found in shallow lakes and ponds (*Platessa hustedtii*, *Stauroforma exiguiformis, Staurosira construens*) in the sand. The fragmentation of diatom valves, and the anomalous tidal flat diatoms and shallow freshwater diatoms in sand bed DW2 are consistent with a tsunami eroding, transporting, and depositing sediments from a variety of environments.

The organic silt immediately overlying sand bed DW2 contains well-preserved, abundant freshwater diatoms and chrysophyte cysts typical of a freshwater marsh environment, similar to sediments below sand bed DW2. No marine taxa were found in samples overlying sand bed DW2.

Sand DW1

Samples from the organic silt below sand bed DW1 (Figure 10) contain well-preserved, abundant freshwater diatoms (*Achnanthidium reimeri, Eunotia praerupta, Pinnularia brevicostata, Pinnularia intermedia*, and *Pinnularia lagerstedtii*) and chrysophyte cysts typical of a freshwater marsh environment. No marine taxa were found in samples underlying sand bed DW1.

Diatoms within sand bed DW1 are characterized by high fragmentation, low concentration, and an influx of marine tidal flat diatoms (*Delphineis surirella* (10%), *Planothidium delicatulum* (10%), *Cocconeis scutellum* (8%)) into an assemblage otherwise dominated by freshwater taxa. We also observed an increase in freshwater diatoms commonly found in shallow lakes and ponds (*Platessa hustedtii*) in the sand. The fragmentation of diatom valves, and the anomalous tidal flat diatoms and shallow freshwater diatoms in sand bed DW1 are consistent with a tsunami eroding, transporting, and depositing sediments from a variety of environments.

The organic silt immediately overlying sand bed DW1 contains well-preserved, abundant freshwater diatoms and chrysophyte cysts typical of a freshwater marsh environment, similar to sediments below sand DW1. No marine taxa were found in samples overlying sand bed DW1.

3.3.2 Dodds Valley

Sand DV4
Samples from the organic silt below sand bed DV4 (Figure 11) contain well-preserved, abundant freshwater diatoms (*Aulacoseira italica, Pinnularia lagerstedtii, Stauroforma exiguiformis,* and *Staurosira construens*) typical of a freshwater peat bog environment with periodic standing water. No marine taxa were found in samples underlying sand bed DV4.

Diatoms within sand bed DV4 are characterized by high fragmentation, low concentration, and an influx of marine tidal flat diatoms (*Surirella ovalis* (4%) and *Planothidium delicatulum* (2%)) and marine plankton (*Thalassiosira* sp. (3%)) into an assemblage otherwise dominated by freshwater taxa. The fragmented, mixed assemblage containing anomalous tidal flat and planktonic marine diatoms is consistent with a marine incursion into the freshwater marsh.

The organic silt overlying sand bed DV4 contains well-preserved, abundant freshwater diatoms typical of a freshwater peat bog environment with periodic standing water, similar to sediments below sand bed DV4. No marine taxa were found in samples overlying sand bed DV4.

Sand DV3
Samples from the organic silt below sand bed DV3 (Figure 12) contain abundant reworked tephra shards and a highly fragmented, low concentration assemblage of freshwater diatoms (*Achnanthidium reimeri, Aulacoseira italica, Eunotia praerupta*, *Pinnularia lagerstedtii, Stauroforma exiguiformis,* and *Staurosira construens*) typical of a freshwater peat bog environment with periodic standing water. The low concentration and high fragmentation of diatom valves in the tephra rich organic silt is probably due to soil forming processes weakening and fragmenting diatom valves. No marine taxa were found in samples underlying sand bed DV3.

Diatoms within sand bed DV3 are characterized by high fragmentation, high concentration, and an influx of marine tidal flat diatoms (*Planothidium delicatulum* (6%), *Cocconeis scutellum* (2%), and marine plankton (*Thalassiosira* sp. (2%)) into an assemblage otherwise dominated by freshwater taxa. The relatively high concentration of diatom valves within the sand bed compared to underlying and overlying tephra rich sediments suggests that the entrainment and rapid burial of diatom valves by the tsunami resulted in higher preservation rates (Hemphill-Haley, 1996; Sawai et al., 2009) than in reworked organic tephras. The fragmented, mixed assemblage containing anomalous tidal flat and planktonic marine diatoms is consistent with a marine incursion into the freshwater marsh.

The organic silt overlying sand bed DV3 contains abundant tephra shards (Red Beard tephra) and a highly fragmented, low concentration of freshwater diatoms typical of a freshwater peat bog environment with periodic standing water, similar to sediments below sand bed DV3. No marine taxa were found in samples overlying sand bed DV3.

Sand DV2
Samples from the organic silt below sand bed DV2 (Figure 12) contain well-preserved, abundant freshwater diatoms (*Aulacoseira italica, Eunotia praerupta*, *Pinnularia lagerstedtii, Stauroforma exiguiformis,* and *Staurosirella pinnata*) typical of a freshwater peat bog environment with periodic standing water. No marine taxa were found in samples underlying sand bed DV2.

Diatoms within sand bed DV2 are characterized by high fragmentation, high concentration, and an influx of marine tidal flat diatoms (*Planothidium delicatulum* (5%), *Cocconeis costata* (2%), and *Delphineis surirella* (2%)) and marine plankton (*Paralia sulcata* (3%)) into an assemblage otherwise dominated by freshwater taxa. We also observed an increase in freshwater diatoms commonly found in shallow lakes and ponds (*Stauroforma exiguiformis, Staurosirella pinnata, Staurosira construens*) in the sand. The fragmentation of diatom valves, the presence of tidal flat diatoms and marine plankton, and the increase in shallow freshwater diatoms in sand bed DV2 are consistent with a tsunami eroding, transporting, and depositing sediments from a variety of environments.

The organic silt overlying sand bed DV2 contains abundant tephra shards and a highly fragmented, low concentration of freshwater diatoms typical of a freshwater peat bog environment with periodic standing water, similar to taxa found below sand bed DV2. No marine taxa were found in samples overlying sand bed DV2.

Sand DV1
Samples from the organic silt below sand bed DV1 (Figure 13) contain abundant reworked tephra shards and a highly fragmented, low concentration assemblage of freshwater diatoms (*Achnanthidium reimeri, Eunotia praerupta*, *Stauroforma exiguiformis, Pinnularia intermedia. Pinnularia lagerstedtii,* and *Aulacoseira italica*) typical of a freshwater peat bog environment with periodic standing water. No marine taxa were found in samples underlying sand bed DV1.

Diatoms within sand bed DV1 are characterized by high fragmentation, high concentration, and an influx of marine tidal flat diatoms (*Planothidium delicatulum* (8%), *Delphineis surirella* (6%), and *Cocconeis scutellum* (3%)) and marine plankton (*Paralia sulcata* (2%)) into an assemblage otherwise dominated by freshwater taxa.

We also observed an increase in freshwater diatoms commonly found in shallow lakes and ponds (*Staurosirella pinnata, Staurosira construens*) in the sand. The fragmentation of diatom valves, the presence of tidal flat diatoms and marine plankton, and the increase in shallow freshwater diatoms in sand bed DV1 are consistent with a tsunami eroding, transporting, and depositing sediments from a variety of environments.

3.3.3 Sandy Bay South

Sand SBS2

Samples from the organic silt below sand bed SBS2 (Figure 14) contain well-preserved, abundant freshwater diatoms (*Aulacoseira italica, Pinnularia intermedia*, *Pinnularia lagerstedtii*, *Stauroforma exiguiformis,* and *Tabellaria flocculosa*) and chrysophyte cysts typical of a freshwater marsh environment. No marine taxa were found in samples underlying sand bed SBS2.

Diatoms within sand bed SBS2 are characterized by high fragmentation, low concentration, and an influx of marine tidal flat diatoms (*Delphineis surirella* (13%), *Cocconeis costata* (3%)) and marine plankton (*Thalassiosira* sp. (3%)) into an assemblage otherwise dominated by freshwater taxa. We also observed an increase in *Platessa hustedtii,* a freshwater diatom commonly found in shallow lakes and ponds. The fragmentation of diatom valves, and the anomalous tidal flat diatoms and shallow freshwater diatoms in sand bed SBS2 are consistent with a tsunami eroding, transporting, and depositing sediments from a variety of environments.

The organic silt immediately overlying sand bed SBS contains well-preserved, abundant freshwater diatoms and chrysophyte cysts typical of a freshwater marsh environment, similar to sediments below sand bed SBS2. We observed fragments of the marine tidal flat diatom *Delphineis surirella* (<2%) in the organic silt immediately overlying sand bed SBS2, likely the result of sediment mixing at the sand-peat contact.

3.4 Geochemistry

Results for all the sediment cores showed BIT index values of ca. 1 suggesting mainly terrestrial OM source. No significant difference was observed between soils from above and below the sand layer in comparison to the tsunami sediment layer. This suggests that the BIT index is not sensitive enough to identify tsunami/storm sediments, the most plausible explanation being backwash from tsunami inundation that entrained terrestrial organic matter within the sand layer and the post-deposition contamination of the sand layer by down profile inwash of peats and root penetration.

4. Conclusions

1. We did not find evidence for land-level changes on Sanak Island. This absence may be due to a lack of suitable recording environments with no extensive salt marshes.

2. Evidence for marine inundation during the 1946 AD earthquake is preserved at multiple sites across southern Sanak, consistent with historical evidence of significant inundation.

3. There is evidence for a further four inundation events prior to the 1946 AD earthquake at four sites across southern Sanak. The sand layers are confirmed to be of marine origin from diatom analysis. We postulate these deposits are a result of tsunami based on lateral extent of deposits and height above modern sea level.

4. Average recurrence interval between tsunami sands was ~675 years between 4300 and 2000 years ago.

5. Geologic evidence suggests a 2000-year gap between tsunami 2 and the 1946 AD earthquake.

6. The relationship between current lack of coupling during the instrumental period and previous marine incursions is unclear.

References

Dawson, S., 2007. Diatom biostratigraphy of tsunami deposits: examples from the 1998 Papua New Guinea tsunami. Sedimentary Geology 200, 328-335.

Denys, L., 1991-1992. A check-list of the diatoms in the Holocene deposits of the western Belgian coastal plain with a survey of their apparent ecological requirements. Ministère des affaires économiques, Service Géologique de Belgique.

Hamilton, S.L., Shennan, I., 2005a. Late Holocene relative sea-level changes and the earthquake deformation cycle around upper Cook Inlet, Alaska. Quaternary Science Reviews 24, 1479–1498.

Hamilton, S.L., Shennan, I., 2005b. Late Holocene great earthquakes and relative sea-level change at Kenai, southern Alaska. Journal of Quaternary Science 20, 95–111.

Hartley, B., Ross, R., Williams, D.M., 1986. A check-list of the freshwater, brackish and marine diatoms of the British Isles and adjoining coastal waters. Journal of the Marine Biological Association of the United Kingdom 66, no. 03, 531-610.

Hemphill-Haley, E, 1995. Diatom evidence for earthquake-induced subsidence and tsunami 300 years ago in southern coastal Washington. Geological Society of America Bulletin 107, 367-378.

Kemp, A.C., Engelhart, S.E., Culver, S.J., Nelson, A.R., Briggs, R., Haeussler, P.J., 2013a. Modern salt-marsh and tidal flat foraminifera from Sitkinak and Simeonof Islands, Alaska. Journal of Foraminiferal Research 43, 88-98.

Kemp, A.C., Nelson, A.R., Horton, B.P., 2013b. Radiocarbon dating of plant macrofossils from salt-marsh sediments. Treatise on Geomophology.

Krammer, K., Lange-Bertalot, H., 1986. Bacillarophyceae 2/1. Naviculaceae, in: Ettl, H., Gerloff, J., Heynig, H., Mollenhauser (Eds.), Süsswasserflora von Mitteleuropa. Gustav Fischer Verlag, Stuttgart, pp. 1–876.

Krammer, K., Lange-Bertalot, H., 1988. Bacillarophyceae 2/2. Basillariaceae, Epithemiaceae, Surirellaceae, in: Ettl, H., Gerloff, J., Heynig, H., Mollenhauser (Eds.), Süsswasserflora von Mitteleuropa. Gustav Fischer Verlag, Stuttgart, pp. 1–600.

Krammer, K., Lange-Bertalot, H., 1991a. Bacillarophyceae 2/3. Centrales, Fragilariaceae, Eunotiaceae, in: Ettl, H., Gerloff, J., Heynig, H., Mollenhauser (Eds.), Süsswasserflora von Mitteleuropa. Gustav Fischer Verlag, Stuttgart, pp. 1–600.

Krammer, K., Lange-Bertalot, H., 1991b. Bacillarophyceae 2/4. Achnanthaceae, Kritische Erganzungen zu Navicula (Lineolatae) und Gomphonema, in: Ettl, H. (Ed.), Pascher's Süsswasserflora von Mitteleuropa, vol. 2, part 4. Gustav Fischer Verlag, Stuttgart, pp. 1–437.

Lander, J.F., 1996. Tsunamis affecting Alaska: 1737-1996. NGDC Key to Geophysical Research, Documentation No. 31, National Geophysical Data Center, Boulder, Colorado.

Lange-Bertalot, H., 2000. Iconographia Diatomologica Annotated Diatom Micrographs – Diatom Flora of Marine Coasts I, Edited: H. Lange-Bertalot; Vol. 7 Pub: Koeltz Scientific Books. Copyright: A.R.G. Gantner Verlag K.G. By: Andrzej Witkowiski, Horst Lange- Bertalot and Ditmar Metzeltin.

Okal, E.A., Plafker, G., Synolakis, C.E., Borrero, J.C., 2003. Near-field survey of the 1946 Aleutian tsunami on Unimak and Sanak Islands. Bulletin of the Seismological Society of America 93, 1226-1234.

Palmer, A.J.M., Abbott, W.H., 1986. Diatoms as sea-level indicators. In: van de Plassche, O. (ed) Sea-level research: A manual for the collection and evaluation of data. Geo Books, Norwich, 435-456.

Parnell, A.C., Haslett, J., Allen, J.R.M., Buck, C.E., Huntley, B., 2008. A flexible approach to assessing synchroneity of past events using Bayesian reconstructions of sedimentation history. Quaternary Science Reviews 27, 1872-1885.

Pilarczyk, J.E., Dura, T., Horton, B.P., Engelhart, S.E., Kemp, A.C., Sawai, Y., 2014. Microfossils from coastal environments as indicators of paleo-earthquakes, tsunamis and storms. Palaeogeography, Palaeoclimatology, Palaeoecology 413, 144-157.

Schouten, S., et al. (2013). An interlaboratory study of Tex86 and BIT analysis of sediments, extracts, and standard mixtures. Geochemistry, Geophysics, Geosystems 14, 5263-5285.

Shennan, I., Long, A., Barlow, N., 2007. Recurrent Holocene paleoseismicity and associated Land/sea-level changes in south central Alaska (U.S. Geological Survey External Grant Award 06HQGR0033). Durham, UK, University of Durham, 39 p., http://earthquake .usgs .gov/research /external /reports /06HQGR0033 .pdf.

Shennan, I., Long, A., Barlow, N., Watcham, E., 2010. Spatial and temporal patterns of deformation associated with multiple late Holocene earthquakes in Alaska (U.S. Geological Survey External Grant Award G09AP00105). Durham, UK, University of Durham, 42 p., http://earthquake .usgs .gov /research /external /reports /G10AP00075 .pdf.

Troels-Smith, J., 1955. Characterization of unconsolidated sediments. Geological Survey of Denmark Series IV, volume 3, no. 10, 73 pp.

Vos, P.C., de Wolf, H., 1988. Methodological aspects of paleo-ecological diatom research in coastal areas of the Netherlands. Geol Mijnbouw 67, 31–40.

Vos, P.C., de Wolf, H., 1993. Diatoms as a tool for reconstruction sedimentary environments in coastal wetlands: methodological aspects. Hydrobiologa 269/270, 285-296

Zong, Y., Shennan, I., Combellick, R.A., Hamilton, S.L., Rutherford, M.M., 2003. Microfossil evidence for land movements associated with the AD 1964 Alaska earthquake. The Holocene 13, 7–20.

Sand Layer	Dodds West	Dodds Valley	Sandy Bay South	Salmon Bay
1	DW1	DV1	-	SB1
2	DW2	DV2	SBS2	SB2
3	DW3	DV3	-	-
4	DW4	-	-	-
5	DW5	DV4	-	-

Table 1. Correlations between site specific sand layers and overall stratigraphic framework for Sanak Island

Event	Site	Sample	NOSAMS	Type	Material	Date + Error	Calibrated	13C
Sand 1	Dodds West	DW107A 7.5-8.5cm	OS-115947	Maximum	Rhizome	155 ± 25	0-284	-26.2
Fine Grey Tephra	Salmon Bay	SB101A 23-24cm	OS-119105	Minimum	Woody stems	1610±130	1297-1812	-28.4
	Sandy Bay South	SBSC2 116.5-117.5cm	OS-115942	Minimum	Stems and Moss	1550±20	1391-1522	-24.4
	Sandy Bay South	SBSC2 119.5-120.5cm	OS-115946	Maximum	Woody stems	1640±25	1418-1610	-26.6
Sand 2	Sandy Bay South	SBSC2 147.5-148.5cm	OS-116171	Minimum	Rhizomes	2120±25	2002-2283	-25.5
	Dodds West	DW107A 30-31cm	OS-116299	Maximum	Woody stems	2320±130	2049-2733	-23.9
	Sandy Bay South	SBSC2 151-152.5cm	OS-116168	Maximum	Cloudberry Seeds	2200±25	2148-2310	-26.9
Coarse Red Tephra	Dodds Valley	DV103A 29-29.5cm	OS-119980	Minimum	Woody stems	2300±15	2318-2349	-24.5
	Dodds West	DW107C 34.5-35.5cm	OS-119688	Minimum	Woody stems	2260±25	2159-2345	-23.7
	Salmon Bay	SB101A 49.5-50cm	OS-115944	Minimum	Bark	130±15	12-269	-27.2
	Sandy Bay South	SBSC2 160.5-161.5cm	OS-119777	Minimum	Twigs	2320±30	2184-2376	-24.9
	Salmon Bay	SB101A 52-53cm	OS-118796	Maximum	Algae holdfasts	3110±20	2455-2747	-17.1
Sand 3	Dodds Valley	DV103A 33-34cm	OS-121226	Maximum	Woody fragments	2570±120	2348-2919	-
	Dodds West	DW107A 36-39cm	OS-116286	Maximum	Moss leaf	Modern	Modern	-27.1
Sand 5	Dodds Valley	DV103C 75.5-76cm	OS-116169	Maximum	Woody stems	3870±25	4183-4412	-26.0
	Dodds West	DW102A 61-62cm	OS-118797	Maximum	Algae holdfasts	4410±25	4083-4403	-17.0
Base of Core	Dodds West	DW102A 65-66cm	OS-118798	-	Algae holdfasts	4420±30	4084-4412	-17.9
Other Dates	Sandy Bay South	SBSC2 129.5-130.5cm	OS-115945	-	Woody stems	1740±20	1572-1708	-24.8
	Sandy Bay South	SBSC2 135-136cm	OS-115943	-	Twigs	1920±20	1822-1920	-26.1

Table 2. AMS 14-C dates used in this study to provide a chronologic framework at Sanak Island

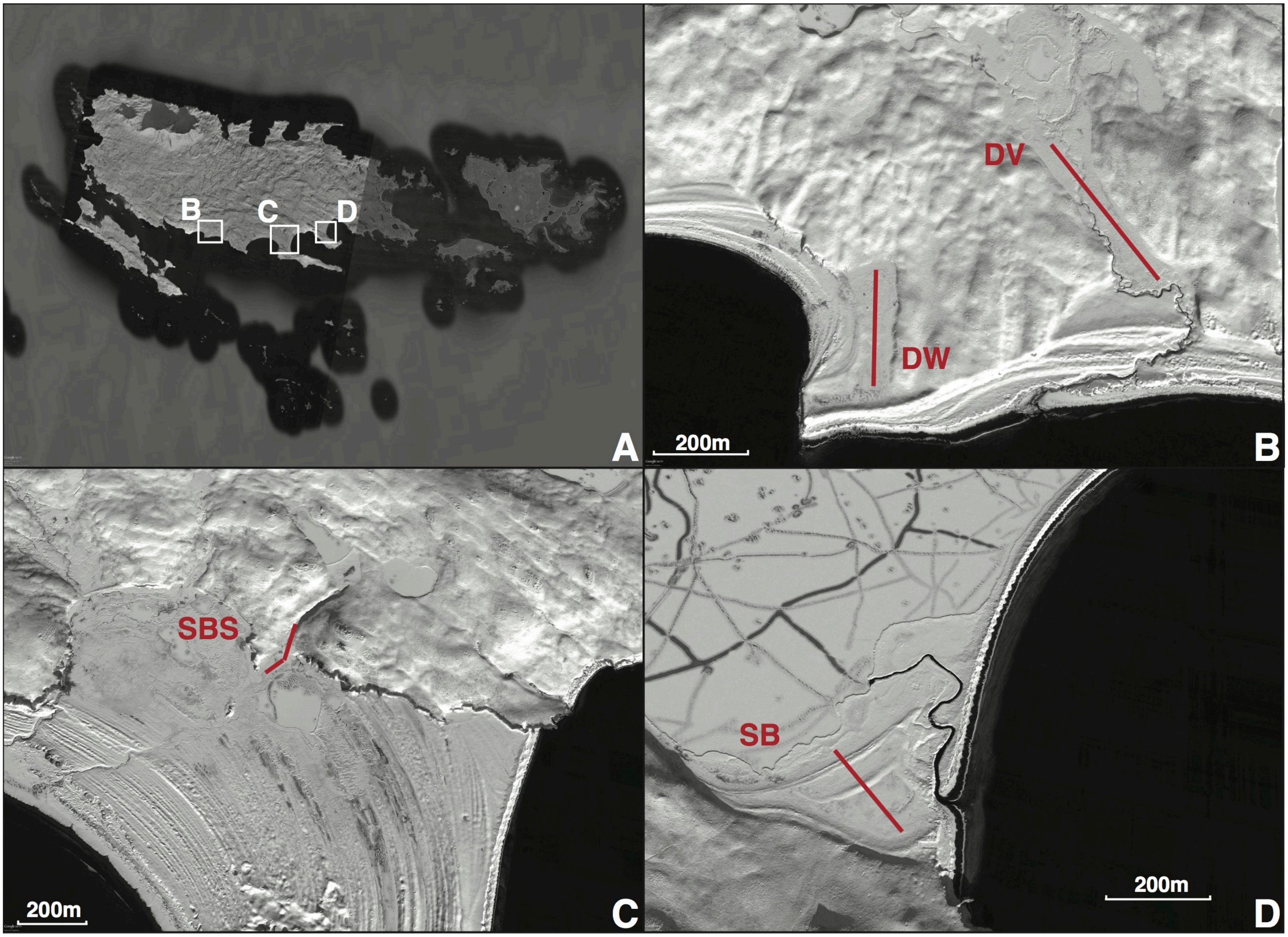

Figure 1. Study area map. A) Sanak Island with three main study sites highlighted by white rectangles. B) Dodds Region study site with Dodds West (DW) and Dodds Valley (DV) coring transects marked by red lines. C) Sandy Bay South site with coring transect marked by red line. D) Salmon Bay site with coring transec marked by red line.

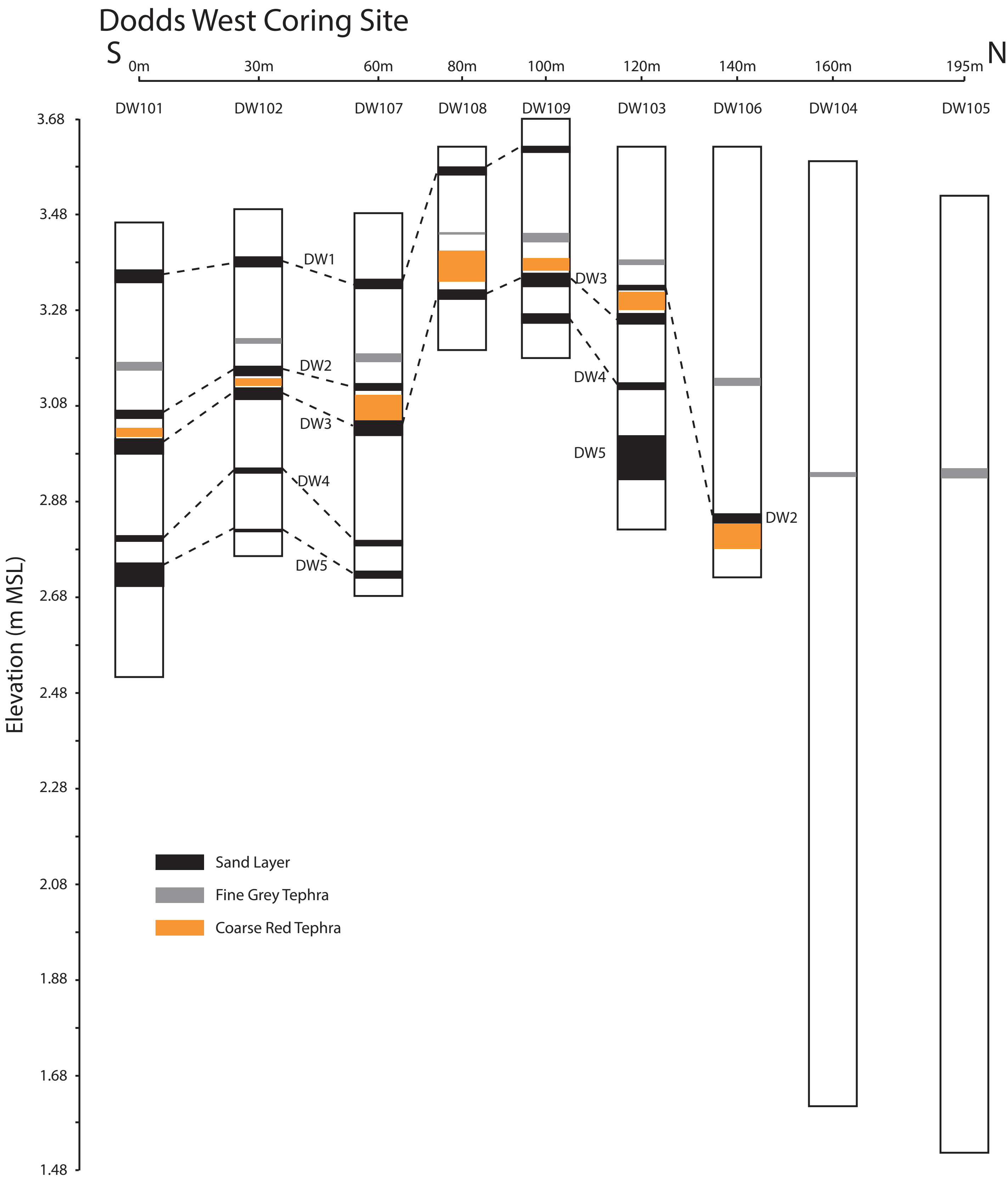

Figure 2. Simplified stratigraphy for Dodds West study site highlighting sand layers and tephras that could be correlated in the field.

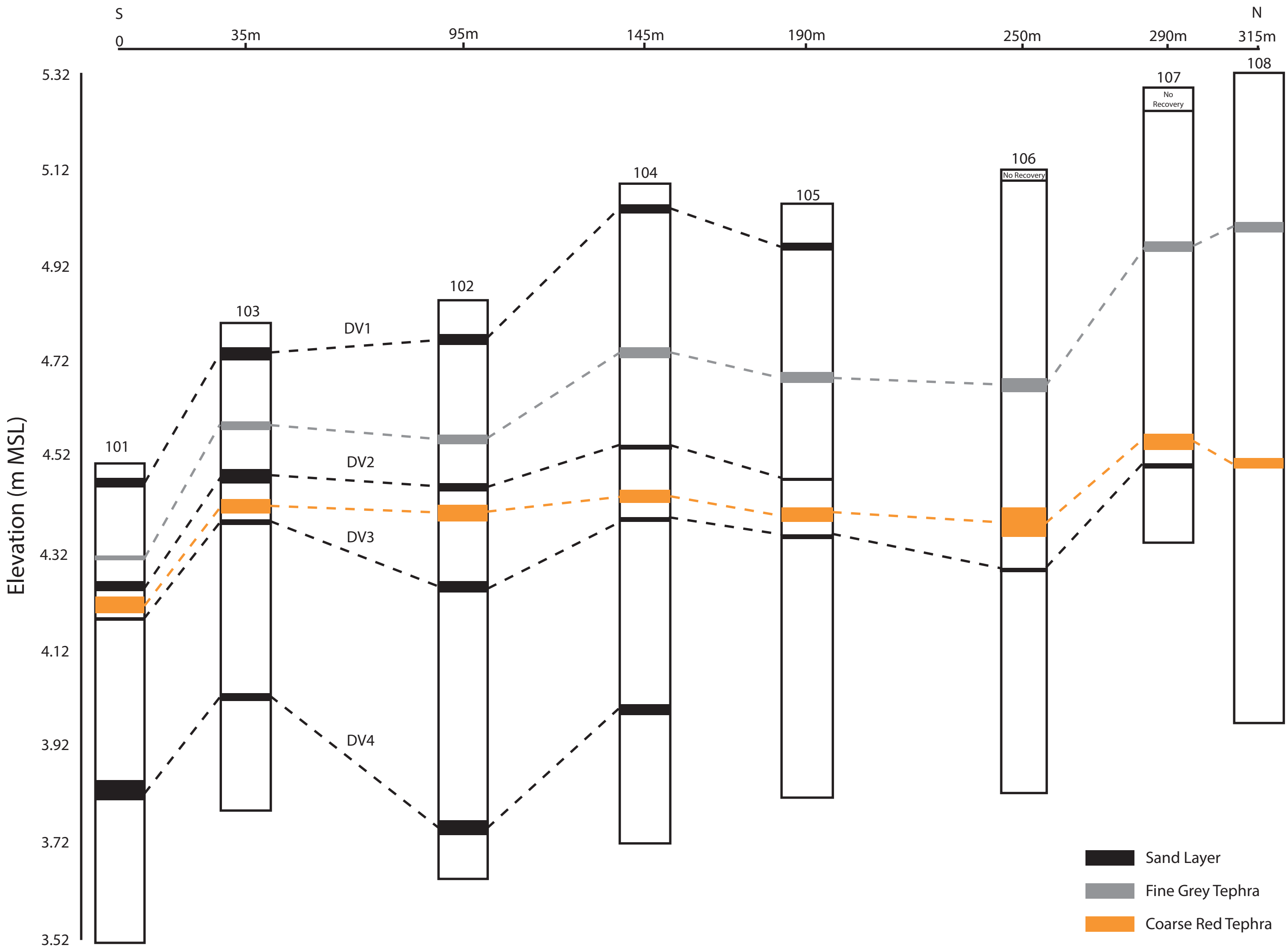

Figure 3. Simplified stratigraphy for Dodds Valley study site highlighting sand layers and tephras that could be correlated in the field.

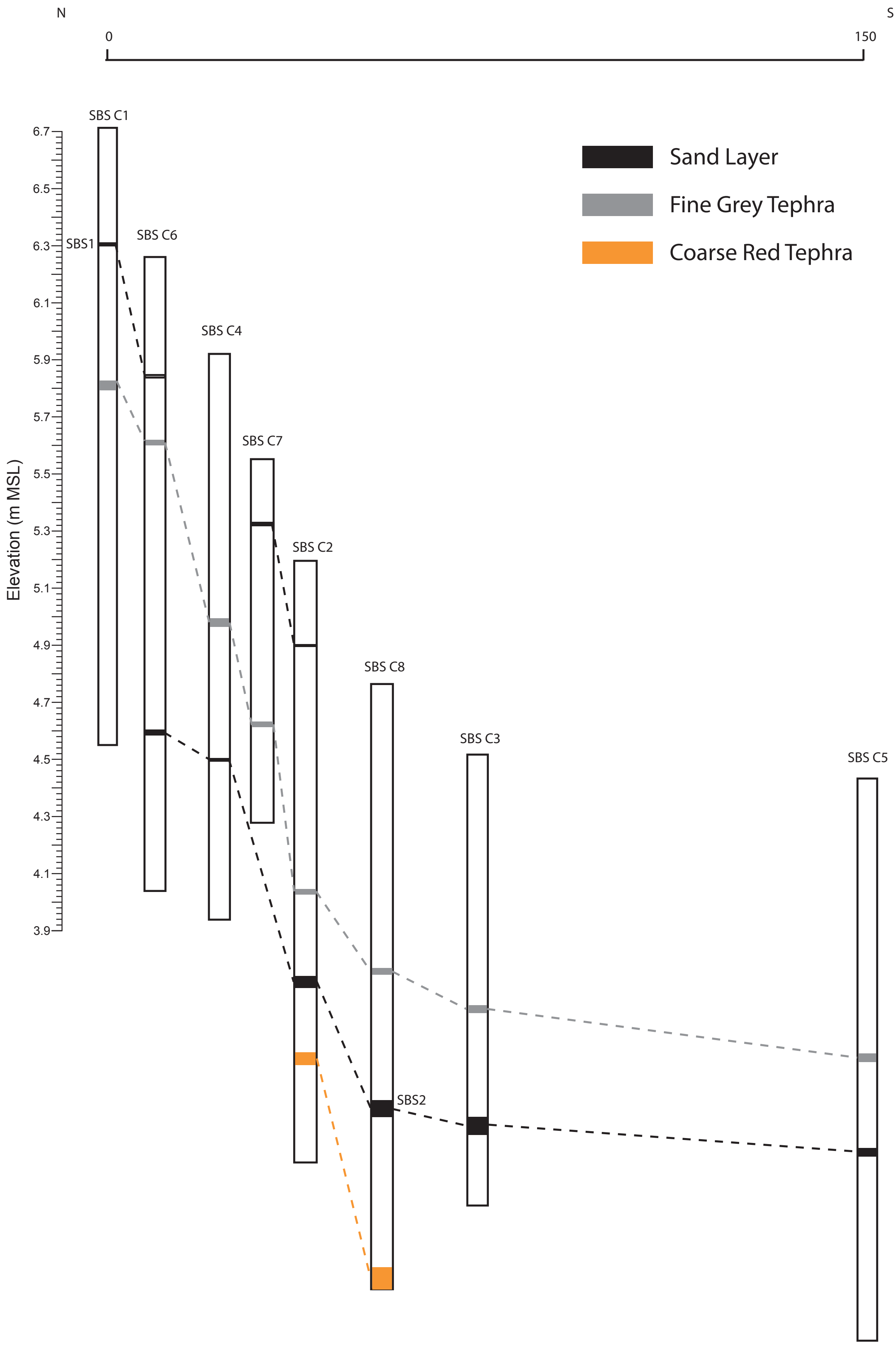

Figure 4. Simplified stratigraphy for Sandy Bay South study site highlighting sand layers and tephras that could be correlated in the field.

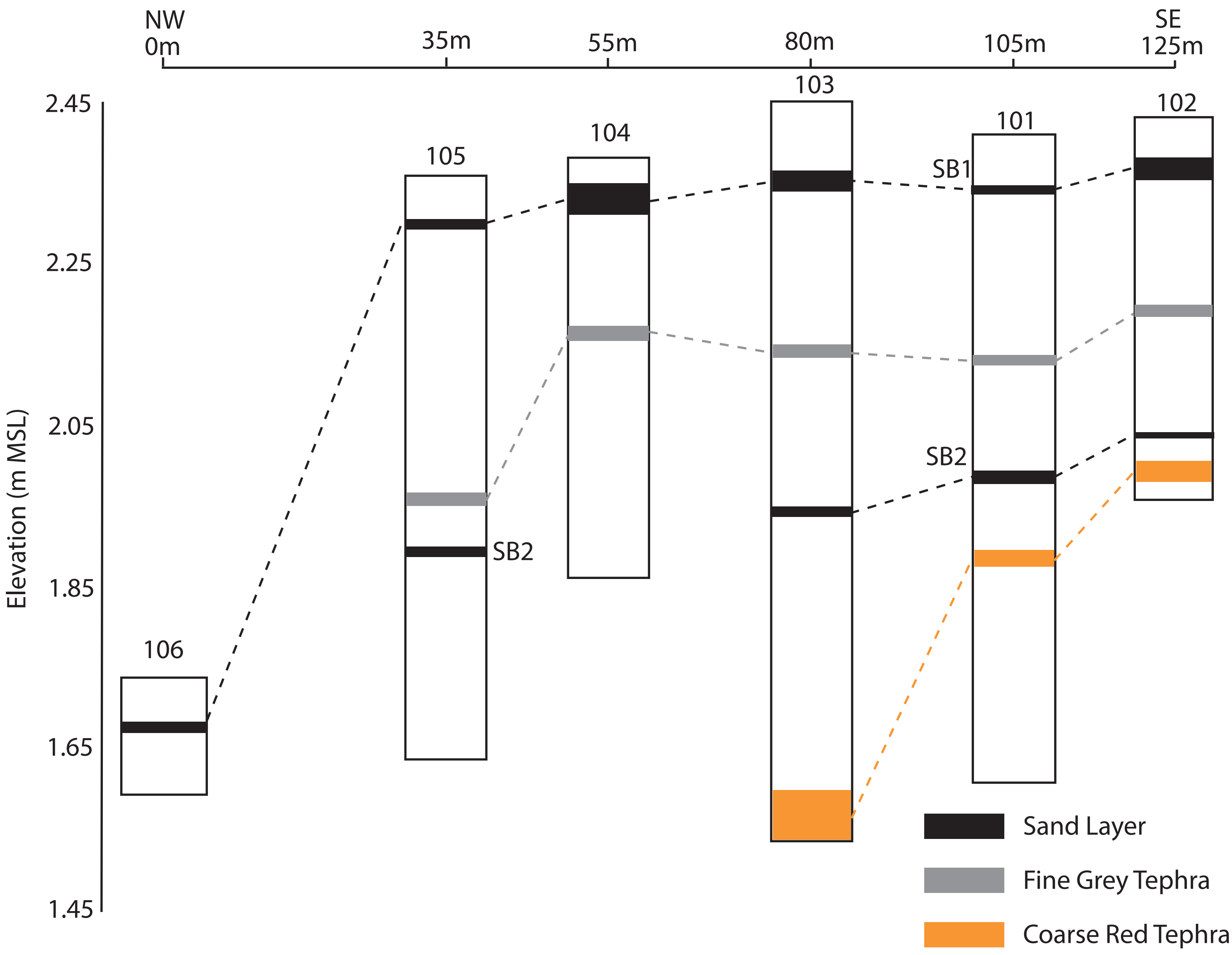

Figure 5. Simplified stratigraphy for Salmon Bay study site highlighting sand layers and tephras that could be correlated in the field.

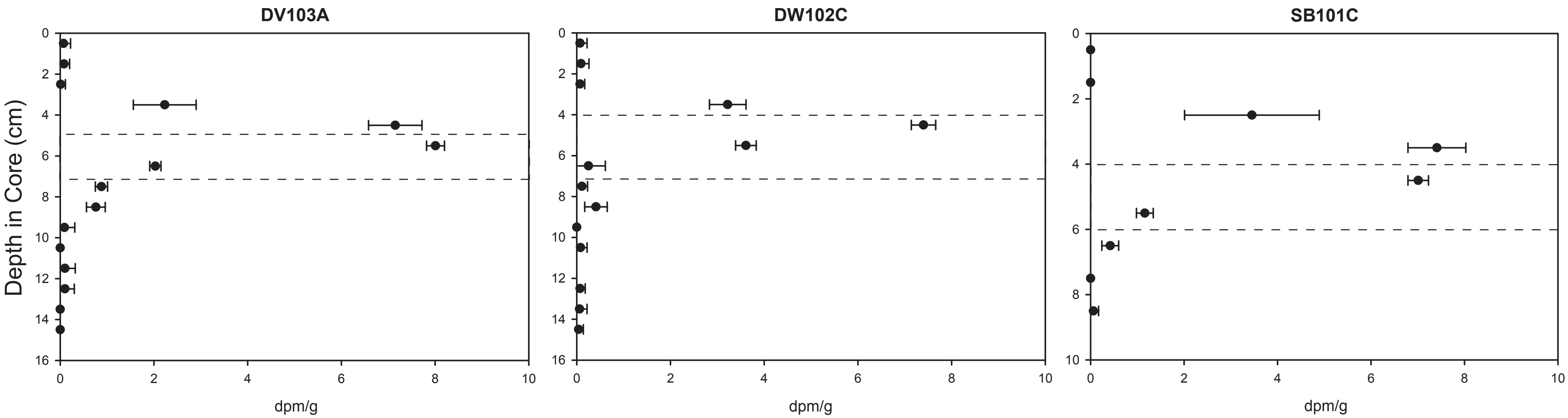

Figure 6. Cesium-137 data for Sand 1 at cores obtained in Dodds Valley (DV103A), Dodds West (DW102C) and Salmon Bay (SB101C) study sites. Cesium-137 distributions identify that Sand 1 at all three sites was deposited prior to 1963.

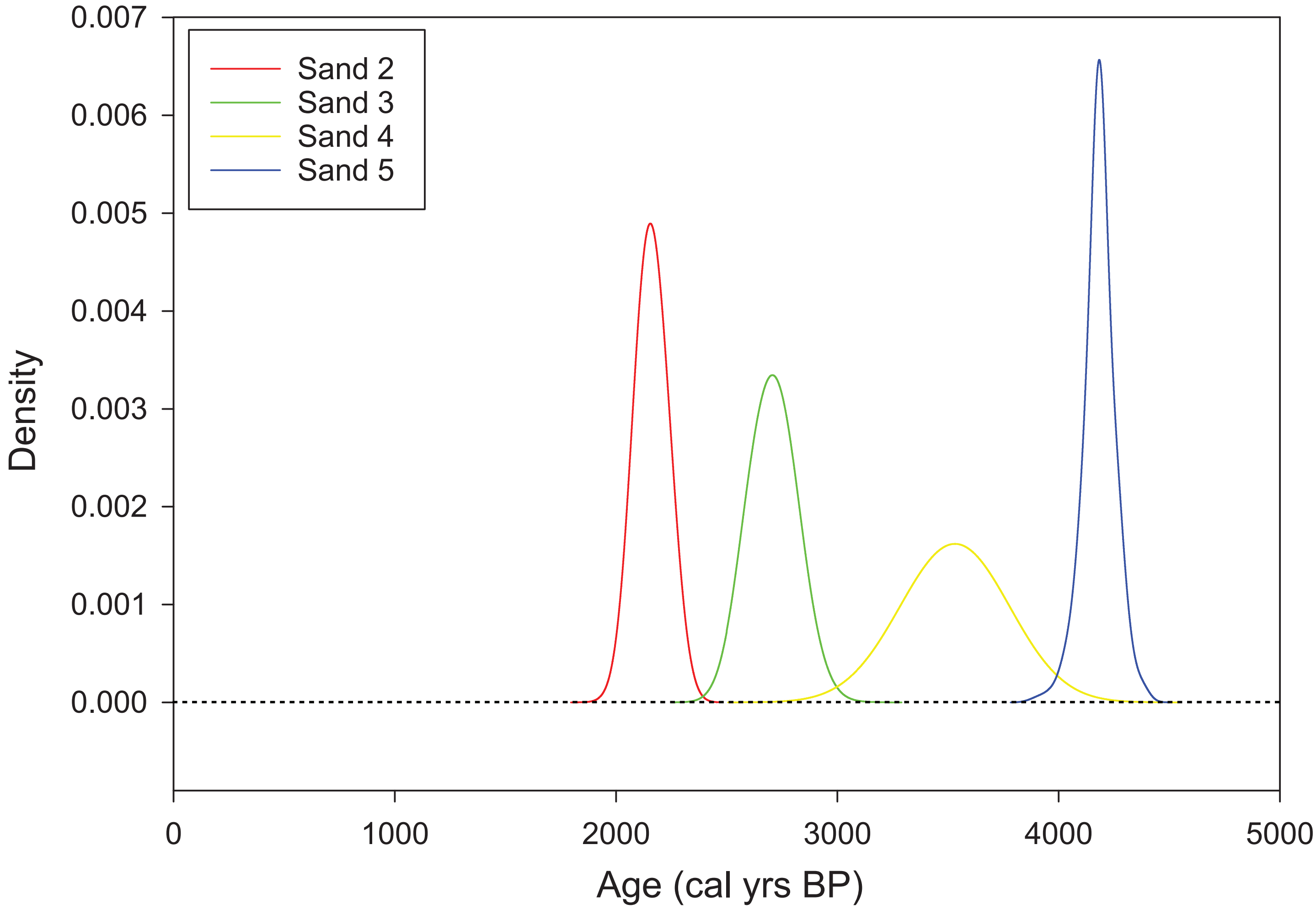

Figure 7. Modeled ages for Sands 2, 3, 4, and 5. Sand ages were modeled using Bchron (Parnell et al., 2008). Sand 4 has a wider age distribution than the other threee sands due to no direct AMS 14-C dates bounding this sand layer.

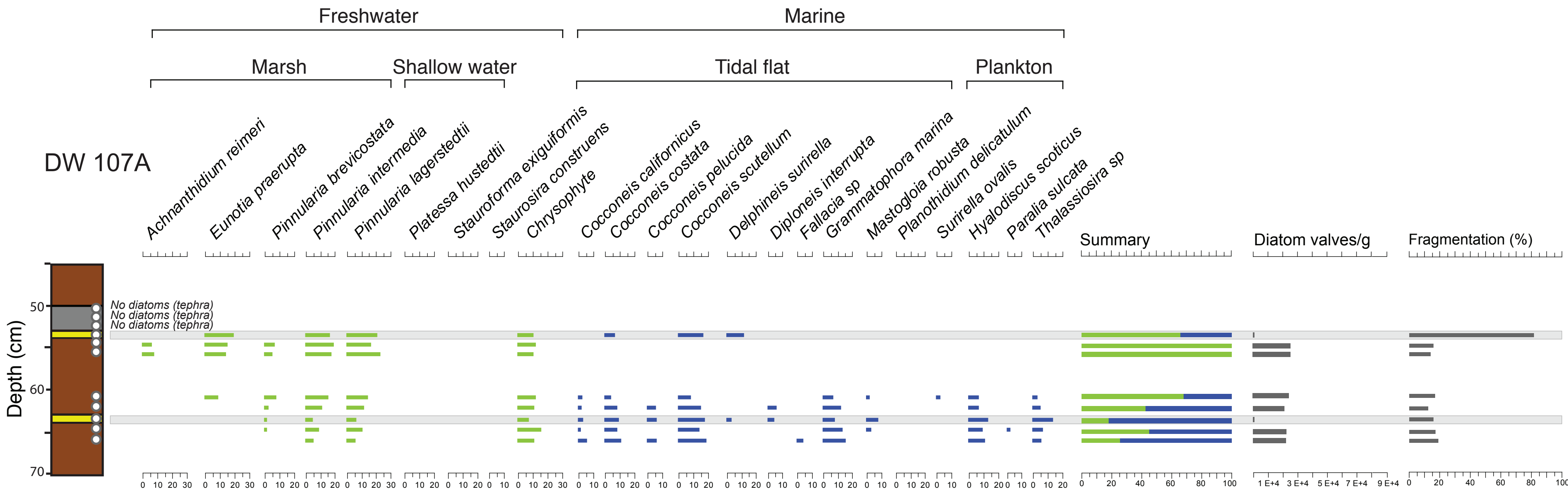

Figure 8. Diatom assemblages for sand layers DW5 and DW4 in Dodds West core DW107A. Diatoms are sub-divided into environmental preference for either freshwater or marine environments. Summary diagrams show the percentage of each environmental preference per sample, as well as the number of diatom valves per gram of sediment, and the percentage of diatoms that were fragmented.

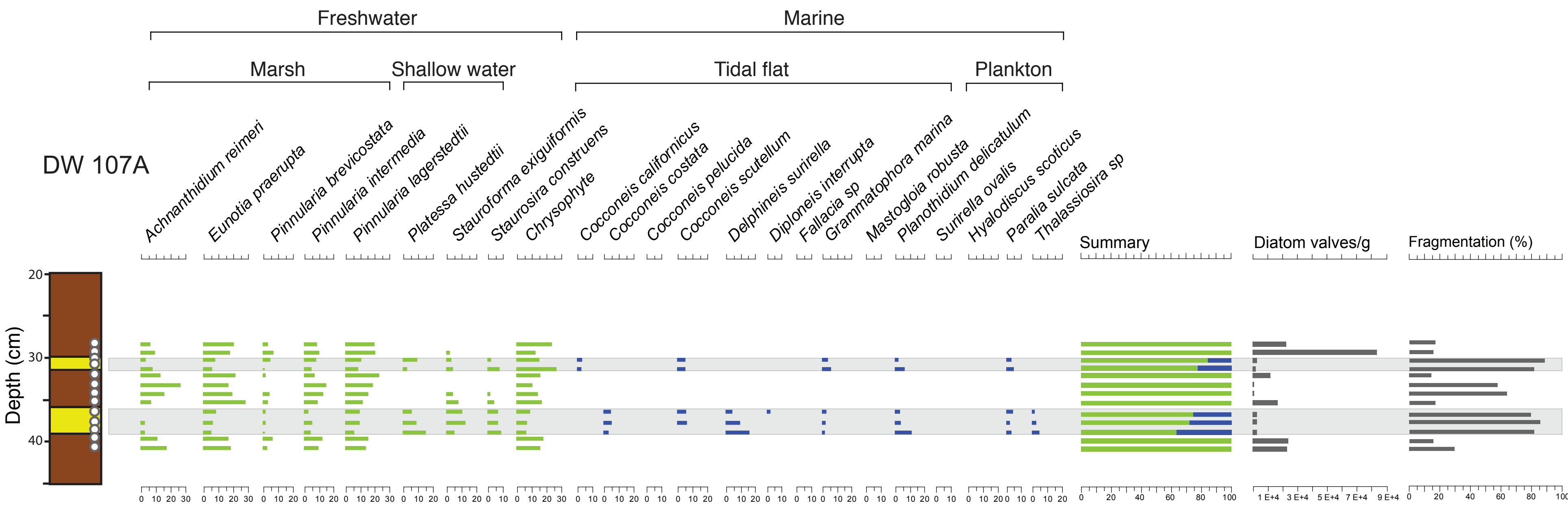

Figure 9. Diatom assemblages for sand layers DW3 and DW2 in Dodds West core DW107A. Diatoms are sub-divided into environmental preference for either freshwater or marine environments. Summary diagrams show the percentage of each environmental preference per sample, as well as the number of diatom valves per gram of sediment, and the percentage of diatoms that were fragmented.

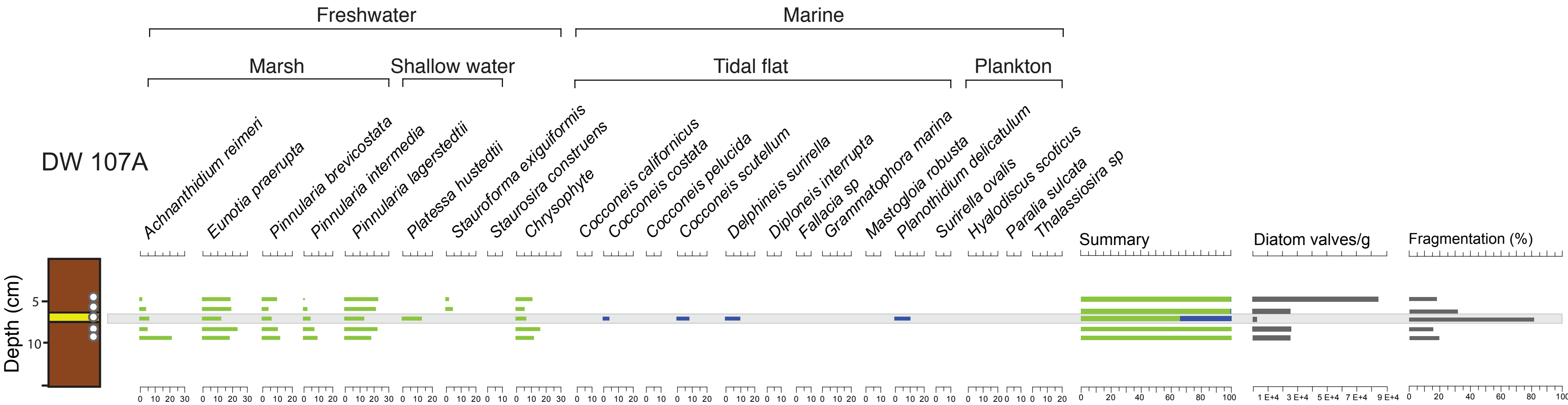

Figure 10. Diatom assemblages for sand layer DW1 in Dodds West core DW107A. Diatoms are sub-divided into environmental preference for either freshwater or marine environments. Summary diagrams show the percentage of each environmental preference per sample, as well as the number of diatom valves per gram of sediment, and the percentage of diatoms that were fragmented.

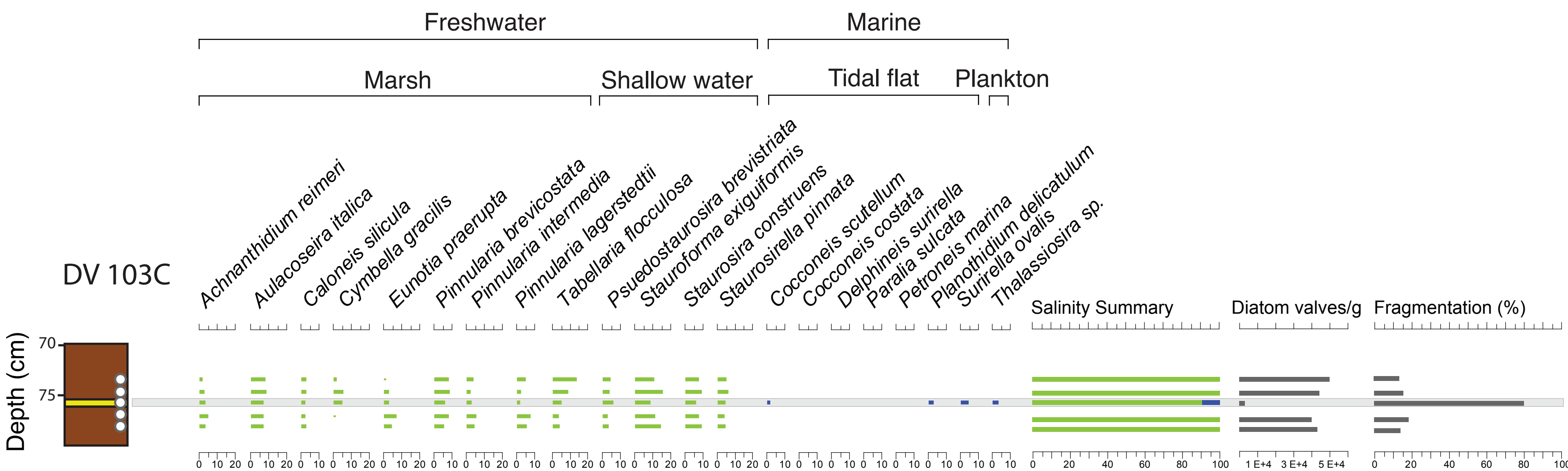

Figure 11. Diatom assemblages for sand layer DV4 in Dodds Valley core DV103C. Diatoms are sub-divided into environmental preference for either freshwater or marine environments. Summary diagrams show the percentage of each environmental preference per sample, as well as the number of diatom valves per gram of sediment, and the percentage of diatoms that were fragmented.

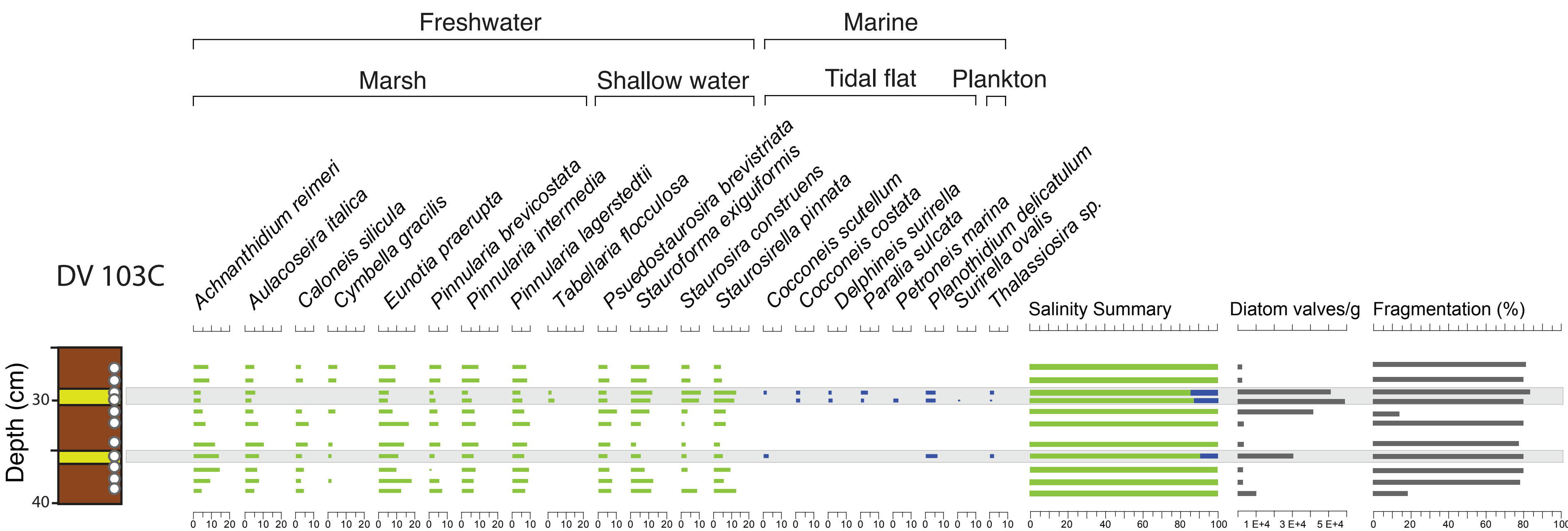

Figure 12. Diatom assemblages for sand layers DV3 and DV2 in Dodds Valley core DV103C. Diatoms are sub-divided into environmental preference for either freshwater or marine environments. Summary diagrams show the percentage of each environmental preference per sample, as well as the number of diatom valves per gram of sediment, and the percentage of diatoms that were fragmented.

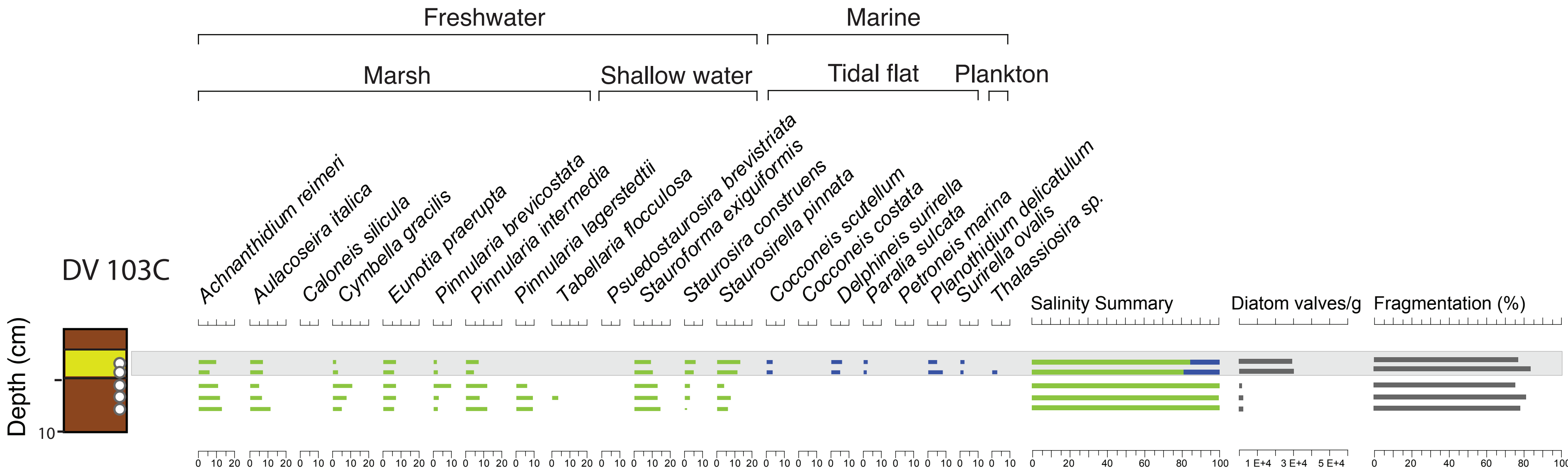

Figure 13. Diatom assemblages for sand layer DV1 in Dodds Valley core DV103C. Diatoms are sub-divided into environmental preference for either freshwater or marine environments. Summary diagrams show the percentage of each environmental preference per sample, as well as the number of diatom valves per gram of sediment, and the percentage of diatoms that were fragmented.

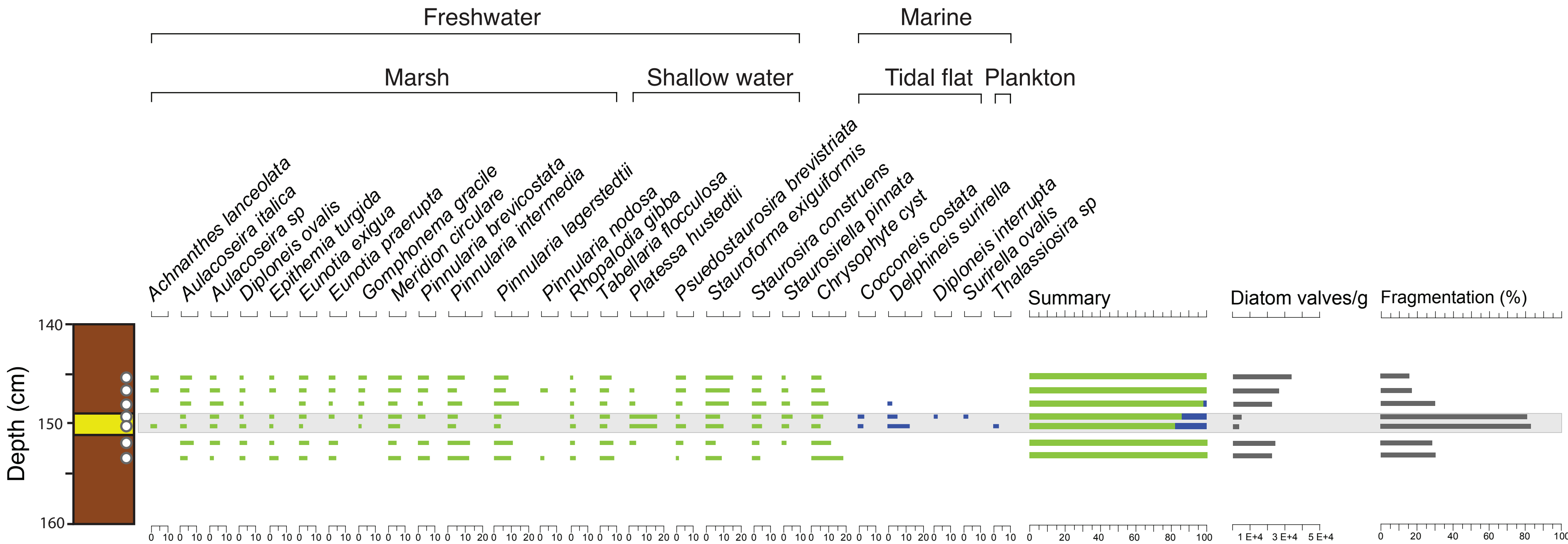

Figure 14. Diatom assemblages for sand layer SBS2 in Sandy Bay South core SBSC2. Diatoms are sub-divided into environmental preference for either freshwater or marine environments. Summary diagrams show the percentage of each environmental preference per sample, as well as the number of diatom valves per gram of sediment, and the percentage of diatoms that were fragmented.